

Suraksha Sharma  
Christoffer A. Bjerk  
Mette Rica Geiker  
Roy Johnsen

# Summary of inspections and investigations on post-tensioning components of Herøysund Bridge, Norway (2017-2023)

Trondheim – January – 2024

## Report

# Summary of inspections and investigations on post-tensioning components of Herøysund Bridge, Norway (2017-2023)

**VERSION**

1

**DATE**

11.01.2024

**AUTHOR(S)**

Suraksha Sharma

Christoffer A. Bjerk

Mette Rica Geiker

Roy Johnsen

**PROJECT NUMBER**

986917104

**NUMBER OF PAGES AND ATTACHMENTS**

13/31

**CLIENT(S)**

Nordlands fylkeskommune

Norwegian Public Roads Administration  
(Statens vegvesen)**ABSTRACT**

This report has been prepared on behalf of the Nordlands fylkeskommune and the Norwegian Public Roads Administration (SVV) and is part of the project "Herøy F&U". SVV has many bridges with similar tension reinforcement that have reached an age and require extensive maintenance. To plan necessary maintenance, inspections, and investigations are quite important.

This report includes results from inspection and investigations carried out on post-tensioned tendons at Herøysund Bridge, including segments of corroded tension reinforcement, ducts, and filler material.

**REPORT NUMBER**

WP2.A2

**ISBN**

978-82-7482-204-7

**CLASSIFICATION**

Open

## Preface and acknowledgements

The report was prepared as part of the Norwegian R&D project Herøysundbru tilstandsevaluering, Herøy FoU (Condition assessment of Herøysund bridge). Funding by Nordland Fylkeskommune and the Norwegian Public Roads Administration is greatly acknowledged.

# Table of Contents

Preface and acknowledgements.....	iii
Table of Contents.....	iv
1. Introduction .....	5
1.1 Objectives.....	5
1.2 Content of the report.....	5
2. Overview of inspections and investigations .....	6
2.1 Bridge overview and naming system .....	6
2.2 Background .....	6
2.2.1 Available reports .....	7
2.2.2 Inspection (2023) .....	7
3. Summary of damages in components of post-tensioned tendons.....	9
4. Summary of results from investigations on components of post-tensioned tendons .....	10
4.1 Filler material .....	10
4.1.1 Chloride content .....	10
4.1.2 Moisture content .....	10
4.1.3 pH of pore water .....	10
4.2 Tension wires .....	11
5. Summary .....	12
6. References .....	13
Appendix A.....	A-1
Appendix B.....	B-1
Appendix C.....	C-1
Appendix D.....	D-1
Appendix E.....	E-1

# 1. Introduction

This report has been prepared on behalf of the Nordlands fylkeskommune and Norwegian Public Roads Administration (SVV) and is part of the project “Herøy F&U”. SVV has many bridges with similar tension reinforcement that have reached an age and require extensive maintenance. To plan necessary maintenance, inspections, and investigations is quite important.

This report includes results from inspection and investigations carried out on post-tensioned tendons at Herøysund Bridge, including segments of corroded tension reinforcement and ducts, and filler material.

## 1.1 Objectives

The objective of this report is to provide an overview of corrosion-related findings from inspections and investigations related to corrosion of post-tensioned wires carried out on Herøysund bridge during the period 2017-2023.

## 1.2 Content of the report

The report has been structured in such a way that all the topics provide a logical connection with each other.

- Chapter 2 gives a background for the report by providing an overview of the bridge and the inspections and investigations carried out.
- Chapter 3 provides the summary of damages witnessed in post-tensioned wires and cable ducts after the concrete removal at specified locations at different time periods. The details of the inspection can be found in Appendix A, B, C, and D.
- Chapter 4 summarizes the results of investigations carried out on the extracted samples of different components of the tendons of the bridge. The details of the inspection can be found in Appendix A, B, C, and D.
- Appendix A provides details of the inspection carried out by SVV and NTNU and investigations carried out by SINTEF and NTNU in 2023.
- Appendix B provides details of the inspection carried out by Multi-consult and Derka in the years 2017 and 2020, respectively.
- Appendix C provides details of investigations carried out on filler material by SINTEF after inspection in October 2019.
- Appendix D provides details of the inspection and investigations carried out by SVV in August 2020 and SINTEF in 2020, respectively.
- Appendix F includes additional images from the inspection done at Herøysund bridge in August 2023.

## 2. Overview of inspections and investigations

### 2.1 Bridge overview and naming system

Herøysund Bridge, with bridge number 18-1069, is located in the municipality of Herøy in Nordland County, Norway. The bridge connects South Herøy with North Herøy and is part of Road FV828. It is situated between HP3/5991 m and 6145 m and was constructed in 1966. This is a cast-in-place beam bridge with varying heights. The bridge consists of 7 spans, including 5 piers and two abutments, with a total length of 154 meters. It has one traffic lane and sidewalks on both sides, with a maximum overall width of 5.30 meters. The main span is 60 meters. The piers and abutments are founded on rock. Each of the two main girders is equipped with four tendons as shown in Figure 2-2.

In this section, two sketches are provided to understand the naming system of where the different inspections have been conducted.

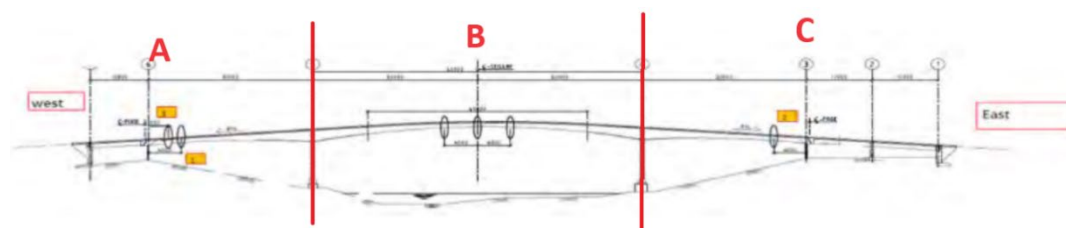


Figure 22-1: Different sections of Herøysund bridge [1].

Figure 2-1 shows the different sections of the bridge. Section A is on the West side of the bridge, section B on the middle span, and section C on the east side.

Figure 2-2 shows the cross-section of the bridge with the four tendons in each beam. The northern side is marked with “N” and the south side with “S”. The different tendon ducts are numbered as shown in Figure 2-2.

To recognize where on the bridge inspections have been done, a naming system is established. An example is: **1SA**. “1” (the number) explains on which tendon duct inspection is done. “S” in the first letter explains if the inspection is on the north or south side. The second letter “A” tells us which section of the bridge (see Figure 2-1).

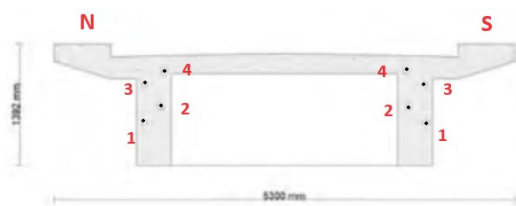


Figure 22-2: Illustration of tendons in the beam [1].

A second example is **2NA**, this inspection is done on tendon duct number 2, on the north side in section A, on the western side.

### 2.2 Background

The inspections and investigations carried out by various organizations have been provided in Table 2-1.

Table 21: Overview of work carried out by different organizations on the bridge.

Work carried	Name of Organization	Date
Inspection	Multiconsult	2017
Investigations of filler material	SINTEF	2019
Inspection	Derka	2020
Inspection	SVV	2020
Investigations of filler material and tension wires	SINTEF	2020
Inspection	SVV and NTNU	2023
Investigations of filler material and tension wires	SINTEF and NTNU	2023

The present report includes a combination of inspections and investigations conducted in 2023 and data from reports from other inspections and investigations referred in Table 2-1.

### 2.2.1 Available reports

The following literature was referred for investigations carried out during 2017-2023. Appendix A, B, C, and D of the present report is translated and rewritten from the following source of documents:

- SINTEF Prøvningsrapport - Laboratorieundersøkelser av injiseringsmasse fra insiden av kabelkanal for spennarmering på Herøysund bru. 2020-03-20.
- SINTEF Prøvningsrapport – Undersøkelser av injiseringsmasse fra kabelbane til Herøysund bru. 2020-11-25.
- Holmqvist, M., Herøysund bridge: Locating voids in grouted tendon ducts with NDT, in Report: Ref. 7204-R-584522-Ver.2 2020, DEKRA Industrial AB.
- NTNU/MTP RAPPORT- HERØYSUND BRU Korrosjon av spennarmering i betongbruer-2022-06-26.
- SINTEF Prøvningsrapport – Undersøkelser av injiseringsmasse fra kabelbane til Herøysund bru. 2023-11-10.

### 2.2.2 Inspection (2023)

Whereas, for the inspections that were carried out on the bridge in 2023, the following tasks (similar to those conducted in 2020) were conducted during the inspection/sampling:

- Photo/video/endoscopic documentation of three sampling areas focusing on the condition of the duct, tension wire, and filler material of the tendon.
- Written documentation of observations for the ducts, tension wire, and filler material.
- Extraction of samples of tension wire, ducts, and filler material for further analysis in the laboratory - in all 10 areas if possible.

Moreover, for marking, storing, and transporting the sample material after extraction, the following procedures were followed:

- Sample pieces of duct, tension wire, and filler material were extracted and stored directly without any cleaning.
- Pieces of tension wire and ducts were placed in plastic bags that were sealed and labeled as per the sampling area. Each bag contained only one type of sample (duct, tension wire, or filler material).
- When a steel surface is exposed to air, it undergoes oxidation due to the presence of moisture in the air. This can potentially change the composition of the passive film or oxide layer on the steel surface once the concrete is removed. Accepting the fact, that silica gel (desiccant) was not used in the storage bags. The sample bags were transported to NTNU for further investigations.

## Summary of investigations

Figure 2-3 illustrates a view of locations where the inspections and investigations were carried out on Section A of the bridge.

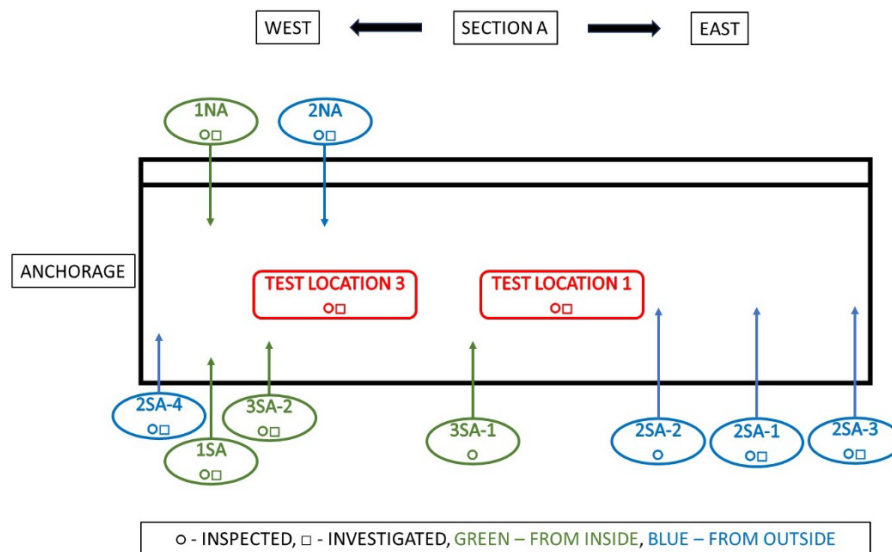


Figure 2-3: Test locations on the bridge: The red areas indicate the inspection carried out in 2020 and the remaining areas are carried out in 2023 in Section A.

Moreover, the type of investigations conducted on the samples at different locations over the period has also been listed in Table 22.

Table 22: Overview of tests conducted on the samples extracted from the bridge over different periods.

Year	Location	Moisture content	XRD	XRF	Thin-section analysis	TGA	Total chloride content	CWE + ICP-MS	pH	Test on wires (SEM/EDS, XRD, and XPS)
2017	NA*						X			
2019	2SA (Test location 3)			X	X		X			
2020	Test location 1	X								X
	Test location 2									X
	Test location 3	X				X	X	X	X	
2023	2SA-1	X	X			X				
	2SA-4	X	X			X	X		X	
	3SA-2	X	X					X	X	
	2SA-3	X	X				X			
	1SA	X	X			X				
	1NA	X	X							
	2NA	X	X				X	X	X	

\*NA: Location not available

### 3. Summary of damages in components of post-tensioned tendons

As the report provides an overview of the condition of several components of post-tensioned tendons including tension reinforcement, ducts, and filler material through inspection and investigations on Herøysund Bridge. Table 3-1 provides a summary of damages in the components at different locations during different time periods by visual inspection. The following chapter in the report includes the details of the inspection and investigations.

Table 3-1: Summary of observed damages in different locations of components of post-tensioned tendons.

Post-tensioned components	Visual observations after removal of concrete	Test location and Year																
		Prior Inspections, Appendix B, C, D							Recent Inspections, Appendix A									
		January 2020			August 2020				August 2023									
		1NC	3S C	2S	1SC	TL-1	TL-2	TL-3	1SA	2SA-1	2SA-2	2SA-3	2SA-4	3SA-1	3SA-2	3SA-16	1NA	2NA
Wire	Wires adhered to filler material			✓	✓	✓	✓			✓					✓		✓	✓
	Surface corrosion					✓		✓	✓	✓		✓	✓	✓		✓		
	Non-uniform and pitting corrosion	✓	✓			✓	✓				✓			✓				
	Wire breakage		✓					✓			✓							
	Presence of loose wires						✓			✓								
Duct	No corrosion		✓		✓		✓										✓	✓
	Internal corrosion	✓				✓		✓	✓	✓		✓	✓	✓				
	External corrosion																	
	Both internal and external corrosion		✓				✓				✓				✓			
Filler Material	Fully grouted			✓	✓				✓				✓		✓		✓	✓
	Presence of voids	✓	✓			✓	✓	✓		✓		✓		✓		✓		
	Moist grout							✓					✓					
	Frost damaged					✓		✓										
	White filler material									✓	✓	✓	✓					
Mild steel	Corrosion	NA	NA	NA	NA	NA	✓		NA	NA	NA	NA	NA	NA	NA	NA	NA	NA
	No signs of corrosion							✓										

\*NA: Not available \*TL: Test location

## 4. Summary of results from investigations on components of post-tensioned tendons

After carrying out the visual observations by removal of the concrete, samples were extracted from the region for further investigations. One corroded and broken tension wire, corroded duct samples, and filler materials were investigated in the laboratory. The results from the analysis from different years have been listed for comparison.

### 4.1 Filler material

The samples of the filler material from specified locations at different periods were analysed. The samples varied in elemental concentration, chloride content, moisture content, and pH and are listed in Table 4-1, Table 4-2, and Table 4-3, respectively.

#### 4.1.1 Chloride content

From the investigations, it can be observed that the chloride content levels determined in the filler material are quite low. In an investigation carried out in 2020 in dry and moist samples, elevated chloride content was observed in moist samples. Conversely, in investigations conducted in 2023, a shift is noted, with higher chloride content generally found in dry samples compared to their moist counterparts.

*Table 4-1: Total chloride content at specified locations at different time periods.*

Year	2020 (January)		2020 (August)		2023 (August)		
Test location	2SA (Test location 3)		Test location 1	Test location 3	2NA	2SA-3	2SA-4
Sample	1	2	Dry	Moist	Dry		Moist
Chloride content (wt %) of filler material	0.036*	0.026*	0.035	0.037	0.061	0.070	0.039

\*of dry weight

#### 4.1.2 Moisture content

In general, the moisture content of moist samples and dry samples greatly varied; the moisture content of moist samples being significantly high. From Table 4-2 it can also be observed that the moisture content differs significantly among test locations; dry samples of Test location 1 (2020) showed higher moisture content than dry samples from 2023.

*Table 4-2: Moisture content of filler material at different locations and time periods.*

Year	2020 (August)		2023 (August)						
Test location	Test location 1	Test location 3	1NA	2NA	1SA	2SA-3	3SA-2	2SA-1	2SA-4
Sample	Dry	Moist	Dry					Moist	
Moisture content (%) of filler material	21.0	44.0	9.2	10.2	13.7	10.2	10.8	25.0	45.1

Note: The moisture content for the year 2017 and for the inspection carried out in January 2020 on Test location 2SA (Test locations 3, 1, and 2), is not available. Hence is omitted from the table.

#### 4.1.3 pH of pore water

From Table 4-3, it can be seen that the pH of the investigated dry samples from 2023 was relatively higher than that of the moist samples. However, the pH of the samples from 2020 was determined

using pH paper which is not as precise as the results from the pH electrode. Hence the value carries some uncertainty.

*Table 4-3: pH of the pore water in different test locations and at different time periods.*

<b>Year</b>	2020 (August)		2023 (August)		
<b>Test location</b>	Test location 1	Test location 3	2NA	3SA-2	2SA-4
<b>Sample</b>	Dry	Moist	Dry		Moist
<b>pH</b>	13*	13*	14.10**	13.76**	12.44**

\*Values were measured using pH paper.

\*\*Values were measured using a pH electrode.

## 4.2 Tension wires

From the study conducted by [2], the fractured wire collected from test location 2SA-2 of the bridge was severely corroded and had 35% reduction in diameter. Moreover, EDS analysis concluded that chloride and sulfur were not present in the corrosion products. The detailed investigations and results carried out on tension wires are provided in detail in [2].

## 5. Summary

This report summarizes the outcome from several inspections and investigations related to corrosion of post-tensioned wires in ducts on the Herøysund Bridge during the period 2017-2023. NDT inspections with different tools, concrete removal followed by closed visual inspection of wires, ducts and filler material, were performed on the bridge. In the laboratory, analysis of the composition of the filler material was performed. In addition, a few corroded and broken wires were examined.

The following conclusion can be drawn:

- Areas with corroded wires inside ducts have been documented. Both “top” and “bottom” wires in the ducts suffer from corrosion.
- Corroded wires have only been found in areas with lack of filler material (partly or complete).
- Three examples of broken wires due to corrosion have been found. Investigations of broken wire samples showed severe corrosion (diameter reduction) in a short distance from the fracture.
- In areas completely filled with filler material, corrosion was not observed on the wires.
- However, even in some areas lacking filler material only shallow surface corrosion (brown surface) was observed on the wires.
- Corrosion was also observed on the duct. In most cases, areas with corroded wires also showed corrosion on the ducts. In some cases, corrosion was documented both on the external and internal surface of the ducts.
- NDT inspection was carried out to identify areas within the ducts that lacked filler material (completely or partly). Concrete removal to inspect ducts and wires, documented in most cases were in good agreement between NDT results and location of filler material in ducts.
- Filler material from selected location from three different inspections were analysed and documented. The most important information regarding corrosion is:
  - Chloride content: 0.026 – 0.070 wt% of filler material
  - Moisture content: 9.2 – 45.1 wt% of filler material
  - pH of pore water: 12.44 – 14.10

## 6. References

1. Johnsen, R., *Herøysund Bru-Korrosjon av spennarmering i betongbruer*. 2022, NTNU: Norway.
2. Bjerk, C.A., *Corrosion of prestressed tensile wires, Herøysund bridge*, in *Department of Mechanical and Industrial Engineering 2023*, NTNU: Norway.
3. Danner, T., *Undersøkelser av injiseringsmasse fra kabelkanal til Herøysund bru - 2023*. 2023, SINTEF: Norway.
4. Danner, T., *Undersøkelser av injiseringsmasse fra kabelkanal til Herøysund bru*. 2020, SINTEF: Norway.
5. Haugen, M., *Prøvningsrapport - Laboratorieundersøkelser av injiseringsmasse fra innsiden av kabelkanal for spennarmering på Herøysund bru*. . 2020-03-20, SINTEF: Norway.
6. Holmqvist, M., *Herøysund bridge : Locating voids in grouted tendon ducts with NDT*, in *Report: Ref. 7204-R-584522-Ver.2* 2020, DEKRA Industrial AB.
7. Holmqvist, M., *Inspection of Herøysund Bridge*. 2023.

## Appendix A : Inspection done by NTNU and SVV (August 2023)

The results for investigations carried out on filler material in Appendix A is rewritten and translated from report [3]. For the fractured wires investigations and results are provided in [2].

Inspection and sampling were carried out at ten test locations in Herøysund Bridge. Inspection procedures along with marking, storing, and transportation of extracted samples were carried out in a similar manner as described in Section 2.2.2.

The following activities, performed both in laboratory and site, were carried out between 2023-08-22 and 2023-11:

- Visual examination, including photo documentation using personal phone and Impact Echo.
- Visual observation after concrete removal.
- Measurement of the relative humidity (Instrument shown in Appendix E)
- Collection of samples for further investigations
- Investigations performed: For filler material (Moisture content, XRD, TGA, total chloride content, CWE+IPC-MS, and pH), for fractured wire (EDS analysis on corrosion products).

### A.1 Documentation of visual observation after concrete removal

The humidity was measured for test locations where voids were present. However, uncertainties prevailed in the measurements. But in all the cases, the relative humidity inside the void was higher than in the atmosphere outside. Other details of observations and investigations performed on all ten test locations are provided below.

#### A.1.1 1SA

##### Observations

Filled up with filler material. Only surface corrosion was observed on wires and duct (inside), see Figure A-1.



Figure A-1: Fully grouted Hole 1SA.

##### Results from investigations

- Moisture content: 13.7% (Provided in detail in Section A.2.2).

#### A.1.2 2SA-1

##### Observations

No corrosion was observed on the external part of the duct, but some surface rust was observed on the inside (brown color), see Figure A-2. The wires were also brown-coloured. However, this was only surface rust since production marks could be seen on the wires.

Filler material (white) covered the gap between the wires but was lacking between the top wire layer and the duct pipe.

Two wires could be moved which indicated that they were broken. The use of an endoscope indicated that more severe corrosion occurred away from the drilled hole. To examine this further, a new hole was drilled 300 mm away (south) of this hole (2SA-2, see Figure A-2).



Figure A-2: Surface corrosion on wires on the top of the duct (Hole 2SA-1).

#### Results from investigations

- Moisture content: 25% (Provided in detail in Section A.2.2).

#### A.1.3 2SA-2

##### Observations

Lack of filler material was observed in the volume between the upper part (1/3) of the wires and the duct.

Serious corrosion on some wires, see Figure A-3. One wire was broken. The fracture was a type of “cope and cone” (On another wire, nearly 40% of the cross-section was corroded away on a length of min. 100 mm (difficult to find the exact length). The distance between the two fractured surfaces was 60 mm.

Corroded duct on the inside.





*Figure A-3: Extensively corroded and fractured wire on top of the duct (Hole 2SA-2).*

#### Results from investigations

As the samples from the filler material from this region were not collected, no further investigations were performed.

#### A.1.4 2SA-3

##### Observations

This point is 2500 mm from 2SA-1 (to the east). Filler material between the wires but was not present between the top wires and the duct, see Figure A-4. The colour of the filler material was white in contact with the wire and the duct and grey for the rest.

Only surface corrosion could be seen on the wires– production marks were also visible.

The internal part of the duct was slightly corroded.

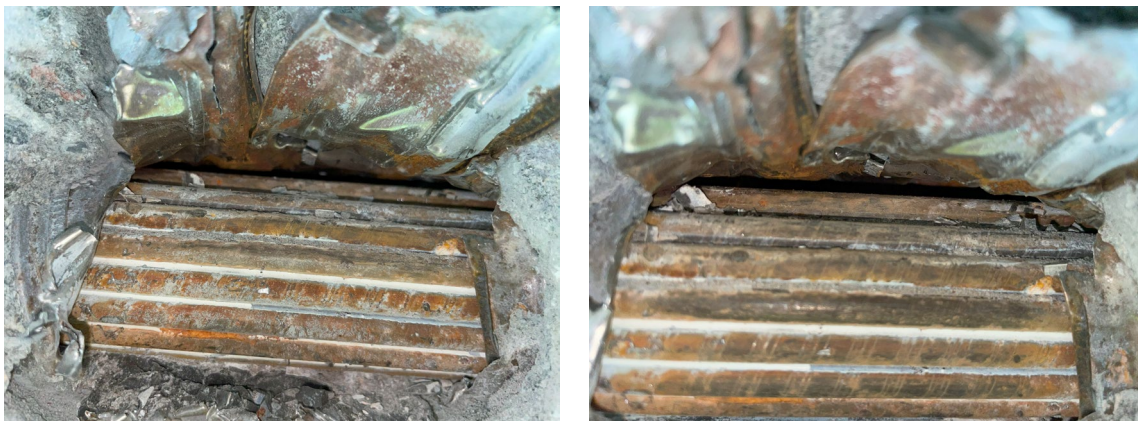


*Figure A-4: Corroded wires along with internal corrosion in the duct (Hole 2SA-3).*

#### Results from investigations

- Moisture content: 10.2%
- Chloride content: 0.070%
- Provided in detail in Section A.2.2.

#### A.1.5 2SA-4

##### Observations

“Wet” filler material covered the wires and the volume between the wires and the duct as shown in Figure A-5.

Only surface corrosion was observed on the wires and production marks were also visible.

Slight corrosion of the ducts on the inside.



*Figure A-5: Wet filler material (Hole 2SA-4).*

**Results from investigations**

- Moisture content: 45.1%
- Chloride content: 0.039%
- pH pore water: 12.44.

Provided in detail in Section A.2.2

**A.1.6 3SA-1**

**Observations**

Fully voided duct with surface corrosion on the wires, but production marks could easily be seen. Indication of some local attacks on the wires located in the bottom of the duct, see Figure A-6.

Corrosion was observed on the internal surface of the duct.



*Figure A-6: Presence of void along with corrosion of tension wires and duct (Hole 3SA-1).*

**Results from investigations**

Due to the lack of filler material from this region, investigations were not performed.

**A.1.7 3SA-2**

**Observations**

The duct was fully grouted, see Figure A-7.

Bitumen tape outside the duct. Some corrosion on the external surface of the duct under the bitumen layer. Internal corrosion on the upper part of the duct.

No corrosion on the wires in the lower part. On the upper part, the wire surface was covered with a layer that was brown coloured. However, scraping this layer indicated that the layer was not due to corrosion. The brown colour was probably due to corrosion on the internal surface of the duct. Production marks could be seen on the wire surface.

The duct was corroded both on the inside and outside.



*Figure A-7: Fully injected duct with corroded tension wires (Hole 3SA-2).*

#### Results from investigations

- Moisture content: 10.8%
- pH in pore water: 13.76
- Provided in detail in Section A.2.2.

#### A.1.8 3SA-16 mm hole

##### Observations

The test hole was drilled with a 16 mm bore hitting approx. the middle of the duct. This was done to compare with inspection results from Inventor.

Through the endoscope, a lack of filler material could be seen in the annulus between the wires and the duct in the inspected area.

Corroded wires were also observed however it was difficult to quantify the attack.

#### A.1.9 1NA

##### Observations

Fully grouted with filler material.

No corrosion was observed – both on the duct and on the wires, see Figure A-8.



Figure A-8: Fully injected duct with no corrosion (Hole 1NA).

#### Results from investigations

- Moisture content: 9.2% (Provided in detail in Section A.2.2).

#### A.1.10 2NA

##### Observations

The duct was fully grouted as shown in Figure A-9.

No corrosion was observed – both on the duct and on the wires.



Figure A-9: Filled with filler material and corrosion of duct only on the overlapping area (Hole 2NA).

#### Results from investigations

- Moisture content: 10.2%
- pH in pore water: 14.1
- Chloride content: 0.061%.

Provided in detail in Section A.2.2.

#### A.2 Investigations on filler material

To investigate the samples of filler material, the samples were divided into two groups according to their appearance.

Group 1 samples appeared to be dry and resembled hardened cement paste with a dark grey colour. Some samples had brown/red-brown spots (2SA-3 and 3SA-2) on the surface of some particles, indicating potential contact with rust. Surface corrosion of tension wires was observed at the location of samples 1SA, 2SA-3, and 2SA-1.

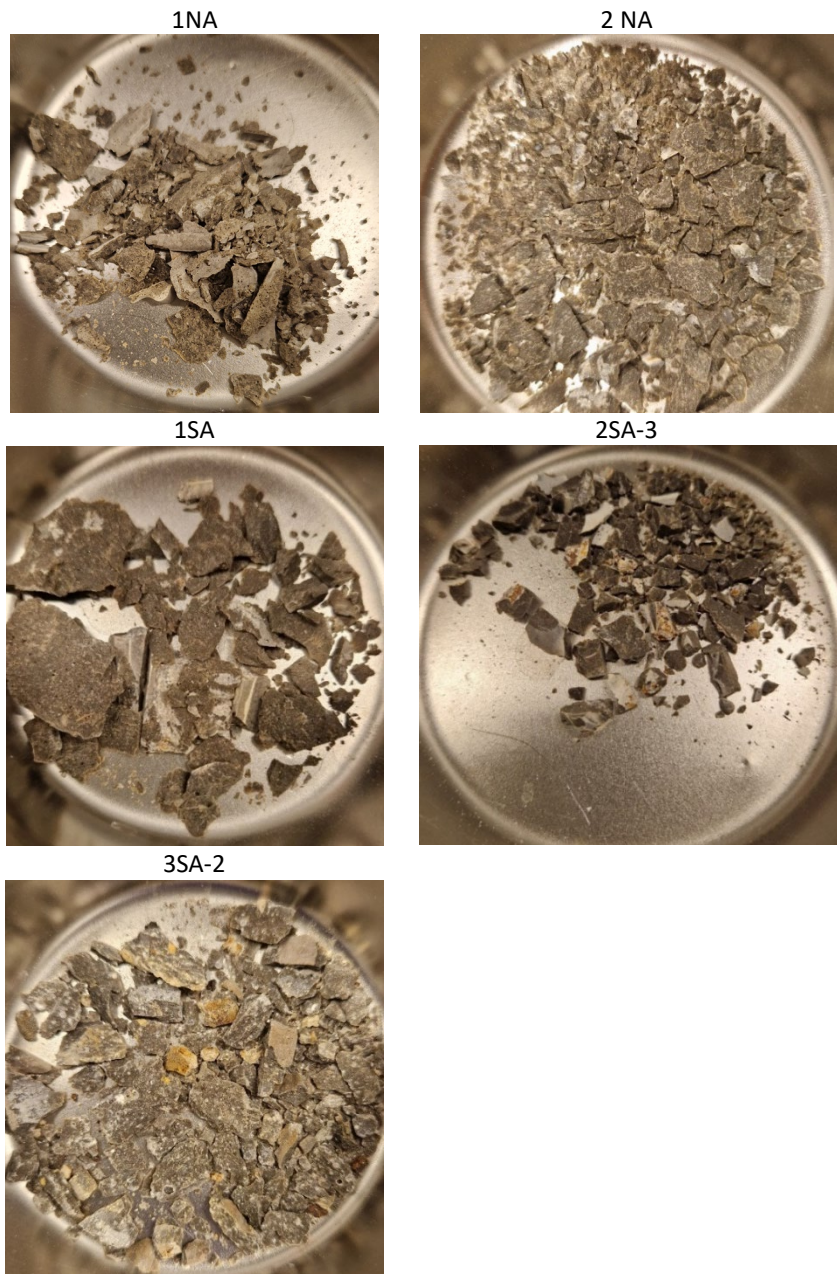


*Figure A-10: Group 1 samples [3].*

Group 2 samples had a lighter colour compared to Group 1 materials, and notably, sample 2SA-4 appeared very moist. Sample 2SA-4 contained a larger piece of metallic material, which was removed before further analysis. The samples also seemed to have lower strength, meaning less resistance to crushing. Group 2 resembled samples received earlier in 2020 [4, 5].



Figure A- 11: Group 2 samples [3].

### A.2.1 Overview of investigations conducted

Table A-1 provides an overview of the conducted analyses for each sample as well as the sample weight upon reception.

Table A-1: Sample weight and summary of conducted analyses [3].

Gruppe	Location	Weight (g)	Moisture	XRD	TGA	Tot. chloride	CWE + ICP-MS	pH
1	2SA-1	1,2	X	X	X			
	2SA-4	6,2 *	X	X	X	X		X
2	3SA-2	8,1	X	X			X	X
	2SA-3	3,6	X	X		X		
	1SA	5,2	X	X	X			
	1NA	5,4	X	X				
	2NA	9,2	X	X		X	X	X

\*Pure sample weight after removal of the metal piece

All samples from Group 1 were hand-ground into fine powder. The samples examined using CWE (Cold Water Extraction) were further ground to  $<80 \mu\text{m}$ . Due to high moisture, it was not possible to grind samples 2SA-1 and 2SA-4 into fine powder, as the powder would only form clumps.

Moisture content analysis was performed through overnight drying at  $105 \text{ }^\circ\text{C}$ . The samples were weighed before and after drying, and the moisture content was calculated in weight percent. The dried sample was discarded, meaning only original samples before drying were taken for further analysis.

X-ray diffraction (XRD) was conducted using a Bruker DaVinci diffractometer. All samples were prepared using the front-loading technique and scanned between  $5\text{-}75 \text{ }^\circ 2\theta$ . Qualitative analysis of crystalline phases was done using DIFFRAC. EVA V4.3 software.

Thermogravimetric analysis (TGA) was carried out with a Mettler Toledo instrument. The samples were initially dried in the TGA instrument for 2 hours at  $50 \text{ }^\circ\text{C}$ . After drying, the samples were automatically heated to  $950 \text{ }^\circ\text{C}$  at a rate of  $10 \text{ }^\circ\text{C}/\text{min}$ . The entire experiment was conducted under an  $\text{N}_2$  atmosphere to prevent potential carbonation.

The total chloride content in the sample was determined according to the SINTEF method for concrete dust analysis (Method 14-05-04-577). The principle involves dissolving the sample in nitric acid, and the chloride content is determined by potentiometric titration with silver nitrate.

Pore water composition was determined using the CWE method (Cold Water Extraction). Unlike the standard procedure (water/sample ratio = 1), about 12 g of water was added to approximately 4 g of dry filler material, thus increasing the water/sample ratio to 3. After 5 minutes of mixing, the sample was filtered, diluted, and neutralized. A complete elemental analysis of the pore water was conducted with ICP-MS at NTNU.

The pH of the pore water was measured from the same solution before dilution and neutralization using a pH electrode. The pH was then calculated back to the pH of the pore water.

## A.2.2 Results from analysis of filler material

### A.2.2.1 Moisture content

Table A-2 shows the moisture content in the samples. Due to the small available sample quantities, moisture content was measured in very small amounts, leading to some level of uncertainty.

The moisture content of samples in group 1 is 10% approx., except for sample 1SA, which has slightly high moisture content (14% approx.).

Moisture content in the samples from Group 2 is significantly higher compared to Group 1. Sample 2SA-4 has a moisture content of 45%, while sample 2SA-1 has 25% moisture. This aligns well with a previously examined sample (Report 3039-282), where 2 samples were received with a moisture content of approximately 21% and 44% respectively.

*Table A-2: Calculated moisture content in the samples from Group 1 and Group 2 [3].*

Group	Sample	Weight before drying (g)	Weight after drying (g)	Moisture content (%)
1	1NA	0.65	0.59	9.2
	2NA	0.49	0.44	10.2
	1SA	0.51	0.44	13.7
	2SA-3	0.49	0.44	10.2
	3SA-2	0.83	0.74	10.8
2	2SA-1	0.2	0.15	25.0
	2SA-4	1.02	0.56	45.1

### A.2.2.2 Total chloride content

Table A-3 provides the total chloride content in samples 2NA, 2SA-3, and 2SA-4. As there wasn't enough material available to conduct measurements on all samples, samples from each group were selected. Sample 2SA-3 was examined since surface corrosion was observed near the extraction site.

*Table A-3: Total chloride content in samples [3].*

Location	2NA	2SA-3	2SA-4
Chloride content (%)	0.061	0.070	0.039

### A.2.2.3 Pore-water analysis

Pore-water analysis was conducted only on samples from Group 1. It is because the method requires the material to be ground down and sieved to <80 µm and this was not possible with samples from Group 2 due to high moisture (2SA-4) or insufficient sample material (2SA-1). However, it is not recommended to oven-dry the samples before analysis as this can significantly impact the pore water quantity and composition through reactions with air and potential partial dissolution of hydrate phases.

In [4] it was discovered that the samples were dried at 105 °C before conducting the CWE procedure and pore water analysis with ICP. This introduces greater uncertainty to these results. Moreover, interpreting the results is challenging as there is no literature available for comparison. The method is

developed for concrete, and the author was not aware of other published analyses conducted on filler material. The results of the current analysis are provided in Table A-4 and Table A-5.

*Table A-4: Results from ICP-MS analysis (mg/L) of filtered solution (pore water) recalculated to the quantity of solution before dilution and neutralization [3].*

(mg/L)	2NA	3SA-2	blank
Na	120.3	19.8	0.01
Mg	0.004	0.006	0.003
Al	0.02	0.02	0.004
S	5.8	1.6	0.002
K	69.9	10.5	0.001
Ca	24.8	63.1	0.12
Fe	0.001	0.003	0.0005
Cl	0	3.2	0

*Table A-5: ICP-MS results converted to mmol/g sample (solid) [3].*

(mmol/g)	2NA	3SA-2	blank
Na	0.016	0.003	0
Mg	0	0	0
Al	0	0	0
S	0.001	0	0
K	0.005	0.001	0
Ca	0.002	0.005	0
Fe	0	0	0
Cl	0	0	0

#### A.2.2.4 PH of pore water

After performing CWE, the pH value was measured using the same solution, before the solution was diluted and neutralized, and subsequently sent for ICP-MS analysis. The sample was mixed with water in a 1:3 ratio (4 g sample + 12 g water) for 5 minutes, then filtered and analyzed. Additionally, the pH was measured in the same way for sample 2SA-4 from Group 1. As there was very little sample remaining, only 1.45 g of sample was mixed with 4.35 g of water. The result is provided in Table A-6.

To convert the pH to pore water, it was assumed that the value from moisture measurement corresponds to free water and therefore pore water.

*Table A-6: The pH value directly measured on filtered solution and converted to pH in pore water [3].*

	2NA (Group 1)	3SA-2 (Group 1)	2SA-4 (Group 2)
Sample (g)	3.999	4.001	1.45
Added water (g)	11.979	11.914	4.35
Porewater (g)*	0.37	0.41	0.65
<b>pH CWE solution</b>	<b>12.58</b>	<b>12.28</b>	<b>11.56</b>
<b>pH of pore water</b>	<b>14.10</b>	<b>13.76</b>	<b>12.44</b>

\*Calculated based on the moisture content in the samples.

#### A.2.2.5 XRD

Figure A-12 displays XRD results from all samples in Group 1. The diffractograms of the samples are very similar regarding the phases present. Presumably, the quantity of different phases is also quite similar in all samples (little difference in the peak heights). They mainly exhibit the presence of portlandite (calcium hydroxide), which, alongside calcium silicate hydrate (CSH), is the primary hydrate phase formed during cement hydration. However, CSH does not have a highly crystalline

structure and thus does not appear in XRD (X-ray amorphous). CSH is only visible as a slight increase in the background level between 25-35 °2θ. Additionally, ettringite (calcium-aluminum sulfate hydrate) is also present. Moreover, small amounts of calcium-aluminum monosulfate (Afm) (to the right of the ettringite peak at 9.1 °2θ) are also observed. Except for sample 2SA-3, there is more ettringite than monosulfate in the samples. Other hydrate phases identified in smaller quantities are calcium-aluminum monocarbonate, katoite, and gibbsite. Additionally, there are small amounts of quartz, calcite, and unhydrated cement clinker phases such as “Alite” and “Belite” (calcium silicate) and calcium aluminate-ferrite.

The samples from Group 2 mostly exhibit similar phases as those of Group 1. However, there are some differences between the samples. Figure A-13 presents a direct comparison between sample 1SA (Group 1) and 2SA-1 (Group 2). It appears that there is more ettringite in Group 2. Additionally, there is more calcite in Group 2, which signifies a reaction with CO<sub>2</sub> from the air (assuming the same cement was used for both samples and therefore the initial calcite content should be the same). The ettringite peaks are not only of increased intensity but also show an asymmetric broadening at higher diffraction angles. From approximately 19 °2θ and upwards, the broadening becomes larger. As a result, there is an additional peak to the right of the ettringite. This could be a possible indication of thaumasite formation in the samples from Group 2.

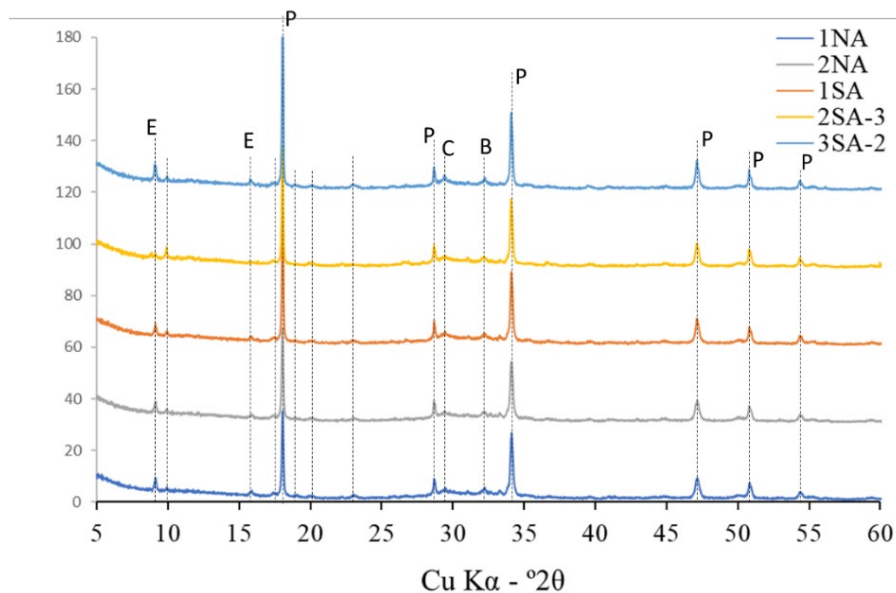


Figure A-12: Stacked diffractograms from Group 1 samples; E = Ettringite, P = Portlandite, C = Calcite, B = Belite (cement clinker) [3].

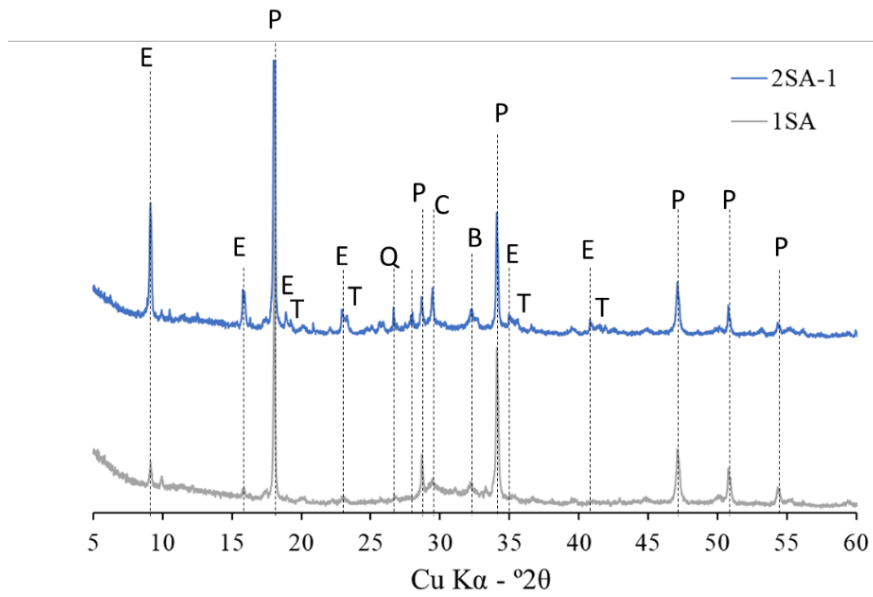


Figure A-13: Stacked diffractograms from Group 1 (1SA) and Group 2 (2SA-1) samples; E = Ettringite, T = Thaumassite, P = Portlandite, C = Calcite, B = Belite (cement clinker) [3].

#### A.2.2.6 TGA

Figure A-14 shows the result from the TGA analysis after drying for 2 hours at 50 °C in an N<sub>2</sub> atmosphere.

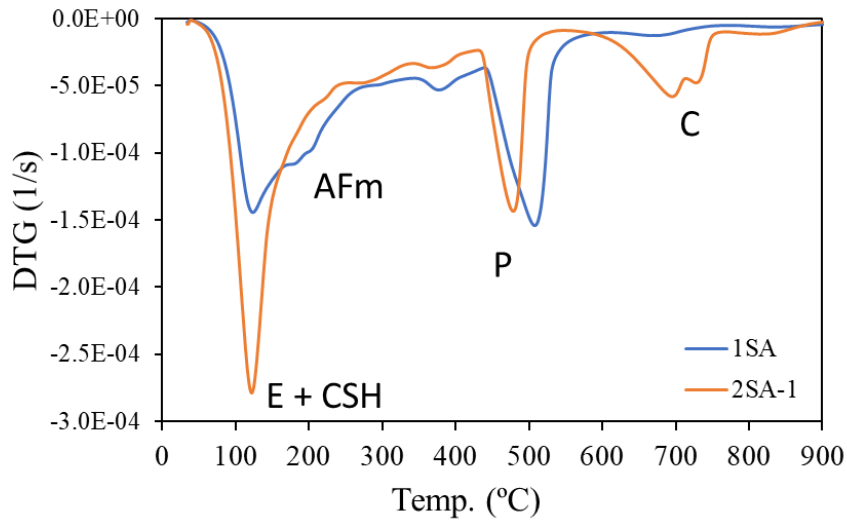


Figure A-14: TGA/DTG analysis of a sample from Group 1 (1SA) and Group 2 (2SA-1) [3].

The results confirm what was found with X-ray diffraction. Samples from Group 2 contain more ettringite (possibly also thaumasite) and more calcite. The width of the portlandite peak (P) indicates higher portlandite content in sample 1SA from Group 1. Calcite formation could be due to exposure to air (carbonation reaction: Portlandite (Ca(OH)<sub>2</sub>) + CO<sub>2</sub> → CaCO<sub>3</sub> + H<sub>2</sub>O), or possibly the addition of limestone filler if this was a separate batch. Ettringite formation (Aft) rather than calcium aluminum monosulfate (AFm) might be due to exposure to moisture and sulfate ions (dissolution and precipitation). As shown, water is also released from the carbonation reaction. To form thaumasite, access to sulfate (SO<sub>4</sub><sup>2-</sup>), carbonate (CO<sub>3</sub><sup>2-</sup>), silicate from C-S-H, and moisture is necessary. Thaumasite formation occurs at temperatures <15°C but is also observed at room temperature (20°C) once it's

formed. Thaumasite isn't hydraulically binding and is known to soften the paste by transforming the typical binder C-S-H.

#### A.2.2.7 Conclusions from investigations

The following conclusions were drawn in the report [3]:

- Samples in Group 1 resembled typical cured cement paste, while Group 2 samples were very moist, relatively soft (partially lumpy), and had a light color typical of undamaged cement paste.
- All samples had low total chloride content, below the threshold considered critical for corrosion initiation.
- Pore water pH was high for all samples. However, Group 1 samples had a higher pH (13-14) compared to the sample examined from Group 2 (12.5).
- Mineralogical analysis with XRD and TGA showed that all samples were well-hydrated, with portlandite and ettringite as the dominant crystalline hydrate phases. However, Group 2 samples had a higher content of calcite and ettringite and a lower content of portlandite. Additionally, there are indications of thaumasite formation in Group 2 samples. Thaumasite is isostructural with ettringite, making it difficult to distinguish between them with XRD. This could explain a possible breakdown of the cement paste (soft mass) and the light color typical in many cases of sulfate attack. To conclusively determine the presence of thaumasite, it is recommended to examine the material with scanning electron microscopy (SEM).

## Appendix B Inspection done by Multiconsult (2017) and Dekra (2020)

Appendix B includes data from [6] and is rewritten and translated from [1].

In 2017, Multiconsult conducted an inspection of Herøysund Bridge on behalf of the Norwegian Public Roads Administration (SVV). The inspection revealed relatively high chloride values (up to 1.89 wt% Cl<sup>-</sup> at depths of 2-10 mm and a minimum cover of 19 mm) were recorded in certain areas.

In January 2020, Dekra conducted an inspection of the tensioning system within the bridge. With various NDT (non-destructive testing) techniques, along with visual observation after removing concrete to access the ducts at four (4) locations of Section C, the following conclusions are provided below [6]:

- Much filler material is missing in parts/areas of the ducts in the bridge's most critical sections.
- Lengths of up to 6 meters with missing filler material were recorded in tendon 3SC.
- Voids indicate the potential for serious corrosion.
- A presumed wire breakage was noted in tendon 3SC.
- Significant variation in corrosion damage to wires in different locations on the bridge.
- The NDT methods used document voids but cannot pinpoint corrosion locations.
- Visual inspection confirmed findings from the use of Ultrasonic and Impact Echo.



Figure B-1: Images by Ultrasonic and Impact Echo (a) Voided duct (1NC) (b) Grouted duct (1SC) [6].

Figure B-1 depicts two examples of visual inspection of ducts and tensioning wires in areas where findings were detected using Ultrasonic and Impact Echo. Figure B-1 (a) was assessed to contain voids (inside the duct), while Figure B-1 (b) was determined to be without voids. This aligns well with what was documented during the visual inspection after the concrete was removed. The visual inspection also documented that both the duct and tensioning wire were subject to corrosion in the area with voids (missing filler material), whereas there were no signs of corrosion (visible brown rust) in fully grouted ducts.

# Appendix C Analysis of filler material done by SINTEF after inspection in October 2019

## C.1 Overview of investigations conducted

Appendix C is translated and re-written from the report [5] and [1].

SINTEF investigated the filler material (consisting of “gravel-like” mass, and iron shavings) of 65 grams retrieved from the inside of the duct (Test location 3 in Figure 2-1, on 2SA towards the anchorage) after an inspection conducted by the Norwegian Public Roads Administration (SVV) in October 2019. After homogenization, the following investigations were carried out between 2020-01-22 and 2020-03-11:

- Chloride analyses (Conducted using potentiometric titration, Methrom titrator, and a silver electrode following SINTEF's internal procedure)
- Elemental determination (XRF analysis was carried out at the Norwegian Geological Survey)
- Thin-section analysis (Microanalysis of a fluorescence-impregnated, polished thin section was examined under a polarization microscope equipped with UV filters)

The key findings from the investigation can be summarized below [5]:

### C.1.1 Chloride Analysis

*Table C-1: Chloride content of samples 1 and 2 [5].*

Sample	Chloride content %
1	0.036
2	0.026

The measured values of the chloride content indicate that the filler material is not significantly mixed with seawater or is contaminated by the ingress of external chloride. As the chloride values are quite low, the risk of chloride-initiated reinforcement corrosion is minimal.

Hence, it cannot be ruled out that frost may have contributed to the degradation of the filler material.

### C.1.2 XRF analysis

The content of the main elements (calcium (Ca) and silicon (Si)) in the fragments of the filler material falls within the range of natural cement as shown in Table C-2. The iron content is high, especially in the 'gravel-like' material probably due to the presence of iron shavings in the sample.

It cannot be ruled out that rust from the tension wires has also migrated into the filler material, thus contributing to the high iron content. Rust in the assumed contact zone with the tension wires can also explain some of the elevated iron content.

*Table C-2: Elemental analysis [5].*

Sample label	Element (wt%)									
	CaO	Fe <sub>2</sub> O <sub>3</sub>	SiO <sub>2</sub>	Al <sub>2</sub> O <sub>3</sub>	MgO	Na <sub>2</sub> O	K <sub>2</sub> O	TiO <sub>2</sub>	MnO	P <sub>2</sub> O <sub>5</sub>
Pieces of filler material	31.7	19.6	10.3	2.71	0.86	0.86	0.436	0.220	0.122	0.042
Gravel like mass	23.2	24.4	16.5	4.22	0.97	0.90	0.548	0.233	0.114	0.051

### C.1.3 Thin section analysis

One fluorescence-impregnated thin section, including 2 pieces of the filler material measuring 45 mm x 30 mm was prepared for analysis as shown in Figure C-1. The results from the analysis as provided in the report are discussed below:

- The analysis of the pieces of filler material shows that the portlandite ( $\text{Ca}(\text{OH})_2$ ) content is very high. The mineral appeared in large quantities in both paste and voids. The absence of visible grains of quartz and feldspar suggested that the material consists of cement paste, not mortar.
- The filler material was found to be highly porous with a very high water/binder ratio, and it is assumed that the mixture has been very fluid.
- Different porosity and grain size were observed between the filler material in the assumed contact zone with tension wires and the remaining part. The filler material layer near the tension wires was slightly more coarse-crystalline and contained some rust.
- It's plausible that this may have happened due to the separation in the material, or the filler material was sprayed in at different times, potentially with slightly different compositions.

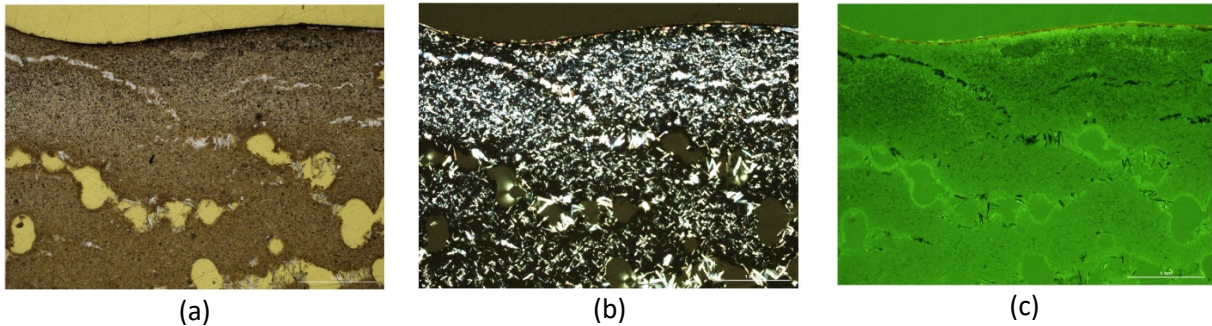


*Figure C- 1: Presumed contact with the duct is at the top part of the image. The filler material appears to be slightly more 'coarse-grained' closer to the duct than further away. (a) Section from thin section (b) Section in polarized light showcasing portlandite by sparkling crystals (c) Section in fluorescent light showcasing rust product on the top and distinction in porosity and grain size approx. in the middle of the image [5].*

## Appendix D Inspection and sampling done by the Norwegian Public Roads Administration (SSV) in August 2020

Appendix D is translated and re-written from the report [1]. The images mentioned in the section can be referred to in “ Vedlegg 5” of the report and are referred to as Bilde nummer [1].

Inspection and sampling were carried out at three predetermined test locations that were previously examined and documented in the Dekra report [6]. Figure 2-1 illustrates the location of Test locations 1, 2, and 3 and Figure D-1 provides a closer look of the locations after concrete removal. Test locations 1 and 3 are 1 m distance apart and are located on the west side of the bridge. Original drawings of tendon placement in the main bridge spans of Herøysund Bridge are shown in Appendix 1 of the report [1]. All the test locations are located on Tendon 2 (Cableway 2N, 2S), but not on the same duct.

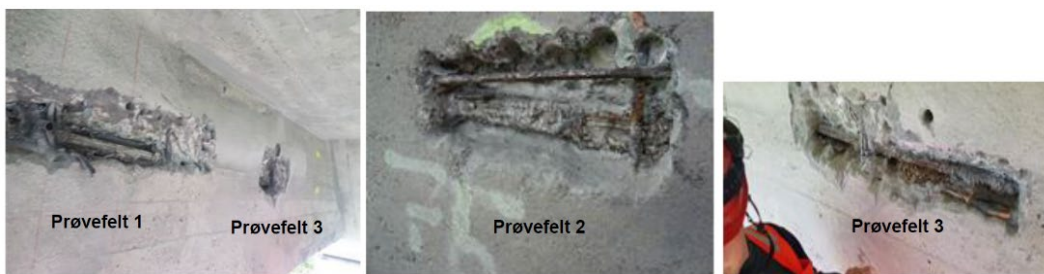


Figure D-1: Inspected test locations [1].

### D.1 Documentation of visual inspection

#### D.1.1 Test location 1

The wires in this location were found to be uniformly corroded in general and the formation of brown rust was observed as shown in the image (1-15) of Figure D-2.



Figure D-2: Photos focusing corrosion (Test location 1) (Image 1-15, 1-16, 1-17, 1-10, 1-9 and 1-12)\* [1].

\*Image names are given as per Appendix 5 in the report [1].

However, near the bottom of the duct, tension wires were observed to be corroded severely, including the formation of pits (Images (1-3, 1-10, 1-16)). The depth and extent of the pits were difficult to quantify as samples were not taken from the area. The attack on one of the wires (1-10) suggests a deep pit with an extent (length) of approximately 2 times the wire's diameter. Some tension wires were fully covered with filler material, preventing corrosion initiation on the wire (1-9). However, it should be noted that the presence of coating on the steel makes it difficult to assess the condition of the steel beneath the coating. In one of the pictures, corrosion products in the form of "black beads" were documented using an endoscope (1-12). Samples of this specific corrosion product were extracted for further analysis.

While assessing the condition of the ducts, images (1-6, 1-7, and 1-8 (Vedlegg 5)) illustrate that filler material adheres internally in the duct around the entire circumference and the condition of the duct is not visible. However, brown rust around the duct can be observed where voids are present. In the image (1-5) (Vedlegg 5), the duct is also visible, but here the internal surface is shiny. The external surface of the duct is shown in image (1-15), and it also appears to be shiny.



Figure D-3: Photos focusing filler material (Test location 1) (Image 1-6, 1-7, 1-11, and 1-3)\* [1].

\*Image names are given as per Appendix 5 in the report [1].

The inspection also reveals the presence of voids in the duct (1-6, 1-7, 1-8 (Vedlegg 5), 1-9, 1-11). From the inspection report carried out by Lise Bathen voids were found to be dry (1-8) (Vedlegg 5) [1]. The consistency of the filler material was found to vary within the inspected area, ranging from normal dry to frost-damaged/non-frost-damaged material. Figure D-4 shows an image of filler material from Test location 1.



Figure D- 4: Filler material from Test location 1 [1].

### D.1.2 Test location 2

After the concrete was removed from the test location, it was observed (Figure D-6: Image (2-2)) that some part of the duct was slightly compressed, indicating the presence of voids in the area. Then the duct was torn up to observe the condition of the tension wires. For Test location 2, it can be seen that some parts of the wires were covered with corrosion products (2-4) (Vedlegg 5), while the remaining parts were covered with adherent filler material (2-7) (Vedlegg 5). In the upper part of the duct, the tension wire was subjected to significant corrosion (2-4, 2-16).



Figure D-5: Photos focusing corrosion ( Test location 2) (Image 2-14, 2-10, 2-15, 2-16 and 2-18)\* [1].

\*Image names are given as per Appendix 5 in the report [1].

The internal corrosion of the duct varied locally. While images 2-10 and 2-16 illustrate substantial corrosion within the duct, images 2-12 and 2-18 show no sign of corrosion. Furthermore, external corrosion of the duct was observed in specific areas (2-16), whereas other areas appeared dull and smooth (2-5).

At this location, mild steel reinforcement in front of the duct was also exposed. The reinforcing steel was mostly intact, with localized surface damage, including some small pits as shown in image 2-14.

One of the tension wires was cut for examination in the laboratory. After it was cut at one end, it retracted about 20 mm (2-8). Then, a length of 350 mm of the tension wire was cut to conduct further analysis at NTNU (2-19) (Vedlegg 5). Loose tension wires (2-15, 2-16) that could be moved with a screwdriver were also discovered in this area.



Figure D-6: Photos focusing filler material (Test location 2) (Image 2-11, 2-12, 2-2, 2-5 and 2-6)\* [1].

\*Image names are given as per Appendix 5 in the report [1].

From the inspection of filler material, it was found that some parts were filled with filler material, but some parts included voids (2-2). The wires covered with filler material showcased full protection from corrosion whereas parts exposed to voids were susceptible to corrosion (2-5). Figure D-7 shows filler material from two areas in Test location 2.



Figure D-7: Filler material from two locations at Test location 2 [1].

### D.1.3 Test location 3

This test location was given priority, and a closer examination was conducted because severe corrosion attacks on the tension wire were observed during the inspection in October 2019. These findings were also documented during this inspection. Additionally, a tension wire that had fractured (Figure D-8: Images (3-2, 3-8 (Vedlegg 5), 3-22, 3-23 (Vedlegg 5)) was discovered. The fracture occurred in wire number 2 from the top as shown in Figure D-9. It can be observed in the image that the fracture in the wire resulted in a gap of 80-90 mm between the fracture surfaces. Pieces of the broken wire were cut - both ends - along with a piece of the nearest tension wire for analysis. Characterization of corrosion attacks, the composition of corrosion products, and analysis of fracture surfaces/areas were analyzed and are presented in Section D.3.1. Moreover, surface corrosion is evident on the wires, as depicted in Figure D-9. It was observed that more corrosion occurred on the wires located at the bottom of the duct. However, it is important to note that the wire with fracture was located at the top of the duct and not at the bottom.



Figure D-8: Photos focusing corrosion (Test location 3) (Image 3-3, 3-16, 3-19, 3-20, 3-21, 3-22, 3-25, 3-2, 3-9)\* [1].

\*Image names are given as per Appendix 5 in the report [1].

In the case of the duct, it was documented that the internal surface was severely corroded (3-4, 3-6) (Vedlegg 5), while the external surface showed no specific signs of corrosion (3-5, 3-6, 3-7) (Vedlegg 5). However, the duct was fully damaged and could be found in pieces as shown in (3-6, 3-7) (Vedlegg 5).

At this location as well, a reinforcing steel in front of the duct was exposed (3-3) but no signs of corrosion were found.

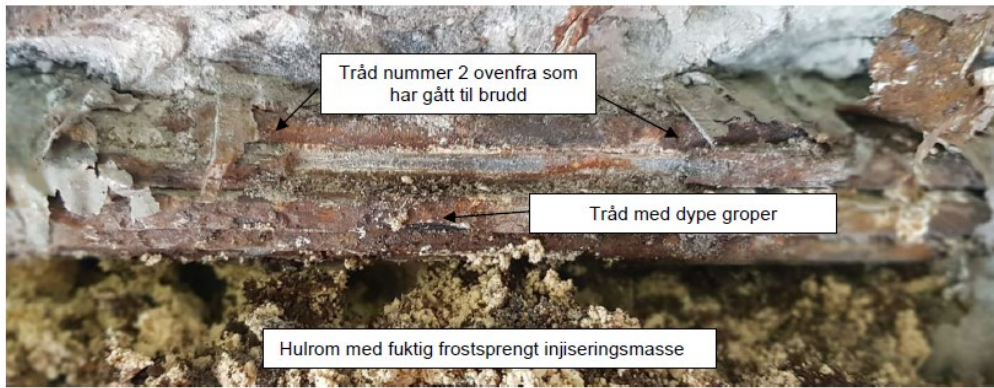


Figure D-9: Tension wire with fractures and other tension wires with deep corrosion pits [1].

Samples of filler material located 20 cm to the east of this location were collected during the inspection in October 2019 and sent to SINTEF for analysis. The consistency of the filler material in this area exhibited noticeable variations, ranging from dry to moist, and from consistent to frost-damaged. Moist and frost-damaged filler mortar was found in the area where a tension wire had fractured, as depicted in Figure D-9. Samples of moist filler material from this area were taken for further analysis at SINTEF. The inspection also documented voids in some parts of the duct (3-6, 3-7) (Vedlegg 5). Some parts of the location contained voids (3-8) (Vedlegg 5), while some parts were fully injected with filler material (3-12). This suggests varying effectiveness/quality of filler material inside the duct.



Figure D-10: Photos focusing filler material (Test location 3) (Image 3-18, 3-2, 3-10, 3-12 and 3-13)\* [1].

\*Image names are given as per Appendix 5 in the report [1].

#### D.1.4 Summary of results from the visual inspections on the bridge:

Based on the visual inspections, the following conclusions were drawn in the report [1]:

- 1 Tension wires are susceptible to corrosion in the presence of voids in the duct and when the filler material does not perform according to specifications.
- 2 Partially severe corrosion was observed on tension wires in all three examined test locations. Both general corrosion and pitting corrosion have been witnessed. Corrosion of wires near the bottom of the duct was more prominent than at the top. Samples of tension wire were collected from two locations and were analyzed in the laboratory (Section D.3.1).
- 3 In one location, a fractured tension wire was found, potentially due to corrosion. Further investigations were carried out in the laboratory.
- 4 The filler material exhibited varying consistency both within and between locations. The filler material appeared to be moister and exhibited different consistency in areas where the most severe corrosion was observed (including wire fractures). This material was further analyzed by SINTEF (Section D.3.2).
- 5 Presence of voids was observed in various locations and was found to be dry.
- 6 Frost-damaged filler material was observed.
- 7 The ducts showcased certain trends:
  - The internal surface was corroded.
  - The external surface showcased no sign of corrosion. This is a particularly important observation as it indicates the existence of a corrosive environment inside the duct but not on the outside.
- 8 In test locations 2 and 3, mild steel reinforcement in front of the duct was exposed. In one location (2), corrosion was observed on the reinforcing steel, while in the other location (3), no corrosion was observed. These observations also corroborate point 7 external corrosion was observed on the duct for Test location 2, while this was not the case for Test location 3.

## D.2 Results from investigations

### D.2.1 Characterization of corrosion damage and wire breakage on tension wires

The corroded tension wires from Test locations 2 and 3 were investigated in the laboratory at NTNU. Part of the investigations was carried out by student Øystein Antonsen as part of his specialization project. The following summarizes the most significant observations and findings.

#### D.2.1.1 Tension wire that had fractured (Test location 3)

Wire segments from both sides of the fracture were examined, and the following observations were made:

- Corrosion damage on portions of the wire on both sides of the fracture.
- Groove-like corrosion attacks were observed in a length of approximately 20 mm on sections of the cross-section, with minimum remaining cross-sectional area (equivalent to 2.9 mm in height).
- Smaller attacks farther away from fracture, with remaining heights in the range of 4.7-5.5 mm.
- Only a part of the circumference was affected by corrosion, while one of the pieces had a significant area that was adhered with the filler material and was not corroded.
- Residual fracture at 45°.
- The remaining cross-sectional area after fracture was estimated to be approximately 30-35% of the original cross-section.



Figure D- 11: Fractured area on the tension wire depicting severe corrosion damage in the vicinity of the fracture area [1].

#### D.2.1.2 Segments of tension wire that were cut out – no fracture (Test location 2)

Corroded tension wire without fractures was cut out from two different positions and taken for examination. Figure D-12 displays images of two wire segments. The following observations were made:



Figure D-12: Photo of corrosion damage on two wire segments. One showcases typical elliptical pits, and other more 'uniform' corrosion on a portion of the circumference [1].

- On one of the 90 mm long segments, there were deep corrosion pits over a length of 50 mm. The pits had an elliptical shape with a length of 5-15 mm, a depth of up to 1.5 mm, and a width of 3-4 mm. All the pits were on the same part of the circumference, while the rest of the circumference showed no signs of corrosion.
- On another 70 mm long segment, uneven and uniform corrosion was observed on one-half of the circumference, with a diameter in the range of 5.9 – 6.1 mm along the entire length of the sample. While no corrosion was observed on the remaining part of the circumference.

The wire segments were also examined using a 3D microscope, where portions of the surface were scanned to document the surfaces. Figure D-13 displays two scanned images of corroded surfaces on a tension wire.

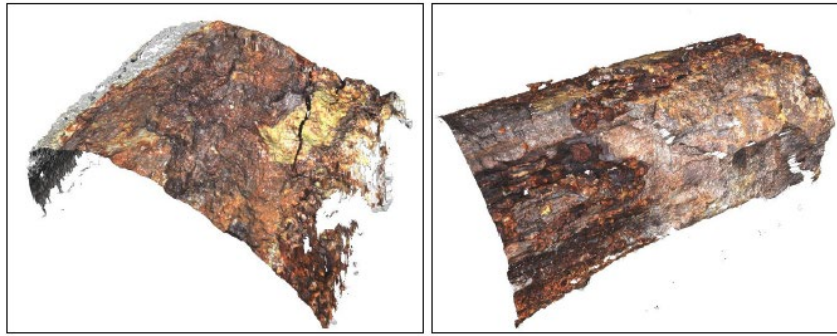


Figure D-13: 3D models of two different areas on a tension wire [1].

Initially, X-ray diffraction (XRD) analysis of the corrosion products was planned to be performed directly on the sample pieces, but considering the suitability of the analysis, it was performed on the scraped corrosion products from the samples. First, the samples were powdered, mounted in a special holder, and then placed into the machine. Figure D-14 displays the result of the XRD analysis in the form of a 'Diffractiongram.' Numerous possible chemical elements/compounds can be witnessed, although some of the peaks are likely due to noise. It is, however, crucial to note that iron compounds with sulfur (sulfide) and chloride are documented, in addition to several Fe-O compounds.

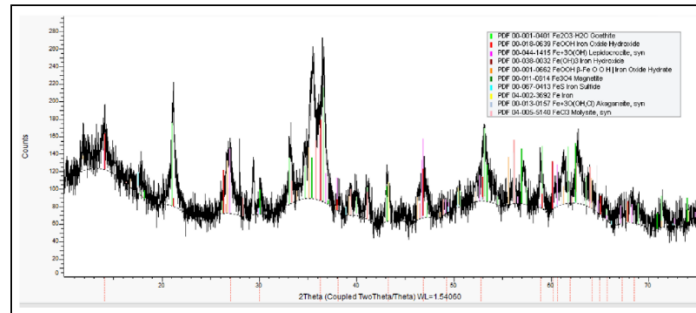


Figure D-14: XRD analysis of corrosion products from corroded wire [1].

Moreover, Scanning Electron Microscopy/Energy Dispersive Spectroscopy (SEM/EDS) was also conducted on corroded tension wires to figure out the chemical elements present on the surface. These analyses also confirmed the presence of both sulfur and chloride on the surface.

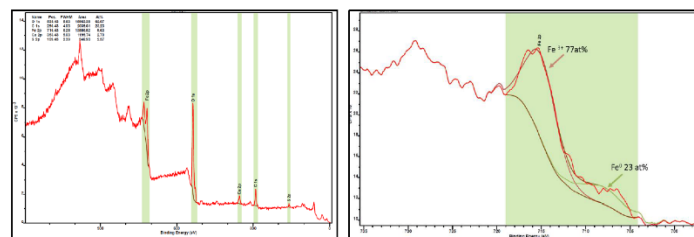


Figure D-15: XPS analysis of corroded wire from Test location 3 [1].

X-ray photoelectron spectroscopy (XPS) analysis was also conducted to analyze the surface chemistry on the corroded tension wire. The results, as shown in Figure D-15, indicate that the surface consisted of O, C, Fe, Ca, and S. A significant amount of trivalent iron ( $\text{Fe}^{3+}$ ) was also detected, as shown in the right figure. This likely originates from  $\text{FeOOH}$  and/or  $\text{Fe}(\text{OH})_3$  compounds. A small amount of sulfur (2.37 at. %) was also detected, while no chloride was found.

### D.2.1.3 Conclusions from the investigation on tension wires

The following conclusions were drawn based on the investigation in the report [1]:

- The examined tension wire from Herøysund Bridge was subjected to corrosion in some parts. Both "uneven" uniform corrosion and pitting corrosion were observed.
- The pits had an elliptical shape with a length of 5-15 mm, a depth of up to 1.5 mm, and a width of 3-4 mm.
- In some sections of the circumference of the wires, "uneven" general corrosion with a depth of up to 0.3 mm was observed, while the remaining part showed no signs of corrosion attack.
- Some sections of the tension wire without corrosion attack were adhered to the filler material.
- The wire that experienced failure exhibited severe corrosion around the fracture area. The remaining cross-sectional area at the time of fracture is estimated to be 30-35% of the original cross-sectional area.
- The remaining fracture appears to be a typical residual fracture due to the material's fracture strength being exceeded as a result of reduced cross-sectional area due to corrosion.
- Examination of corrosion products using SEM/EDS, XRD, and XPS yielded the following results:
  - SEM/EDS and XRD: Sulphur and chloride
  - XPS: Sulphur

### D.2.2 Analysis of filler material

The filler material from Test location 1 (referred to as the 'dry sample') and from Test location 3 (referred to as the 'moist sample') as shown in Figure D-16 was analyzed by SINTEF. Detailed results are described in [4].



Figure D-16: 'Dry' (left) and 'moist' (right) filler material [4].

#### D.2.2.1 Moisture content

Visually both the samples look similar, however, the moisture content in the filler material varies greatly and is summarized in Table D-1. The samples contained a 'gravel-like' grey mass, as well as partially corroded metallic fragments and some darker fragments. An attempt was made to remove the metallic fragments with the help of magnetic rods and tweezers.

Table D-1: Moisture content in the filler material (Test location 3) [4].

Sample	Moisture content (weight %)	Moisture content adjusted for removed metal and rubber mass (weight %)
Dry Sample	18	21
Moist Sample	39	44

#### D.2.2.2 Pore-water composition

For the pore water from the CWE (Capillary Water Extraction) analysis, a pH value of 13 was measured for both samples using pH paper. This falls within the typical range for pore water from Portland cement, mortar, or concrete. However, the method is not as precise as a pH electrode, so the value carries some uncertainty. Results from the pore water analyses are provided in Table D-2.

Table D-2: Composition of pore water in the filler material (Test location 3) [4].

Element	Moist Sample (mmol/L)	Dry Sample (mmol/L)	Moist Sample (mmol/g dry material <sup>1</sup> )	Dry Sample (mmol/g dry material <sup>1</sup> )
Na	43.406	1.982	0.130	0.006
K	13.088	1.070	0.039	0.003
Ca	5.729	15.361	0.017	0.046
Al	0.01	0.01	<0.01	<0.01
Si	0.046	0.030	<0.001	<0.001
Fe	0.002	0.001	<0.001	<0.001
Ti	<0.001	<0.001	<0.001	<0.001
Mg	0.001	0.001	<0.001	<0.001
S	8.999	1.138	0.027	0.003
Cl	0.677	0.536	0.002	0.002

<sup>1</sup> Sample dried at 50°C.

### D.2.2.3 Composition of dry matter

#### TGA analysis

Moreover, the composition of the dry matter in the filler material (dried (50°C) and ground samples) was also analyzed using thermogravimetric analysis (TGA). The results are provided in Table D-3.

Table D-3: Composition of dry matter in filler material (Test location 3) [4].

Parameter	Dry Sample (weight%)	Sample (weight%)
Bound water in the range of 100-350°C	15	23
Total bound water in the range of 100-550°C	20	30
Portlandite	17	23
Calcite	18	17
Ignition loss at 900°C	24	29

### D.2.2.4 Chloride Content

The chloride content of the filler material was also examined and presented in Table D-4. The chloride content was nearly equal in both samples. This indicates that the filler material has not been exposed to seawater from outside. The results are coherent with the samples from the 2019 inspection.

Table D-4: Total chloride content in dry and moist filler material [4].

	Dry sample	Moist sample
Chloride content, %Cl <sup>-</sup>	0.035	0.037

### D.2.3 Conclusions from investigations on filler material [4]

- There is a low probability of external environmental influence (outside the duct) on the filler material based on the following observations:
  - Low total chloride content in the solids and low chloride content in the pore solution (from the CWE analysis).
  - Likely little to no carbonation of the samples.
  - No signs of leaching of cement paste in the moist sample (but possibly some leaching in the dry sample).
- Observed differences between the dry and moist samples and the general condition of the filler material, tension wires, and duct are due to uneven and partially insufficient mixing of the filler material, as well as probable exposure to water in the duct due to separation and possibly the water used for lubrication. It appears more likely that frost exposure due to free water in the duct and natural temperature variations throughout the year are the reasons for

the condition of the filler material and duct, rather than influence from the external environment (sea or rainwater).

## Appendix E Images from inspection 2023



Figure E-1: Instrument used to measure moisture.



Figure E-2: 2SA-1 [7].

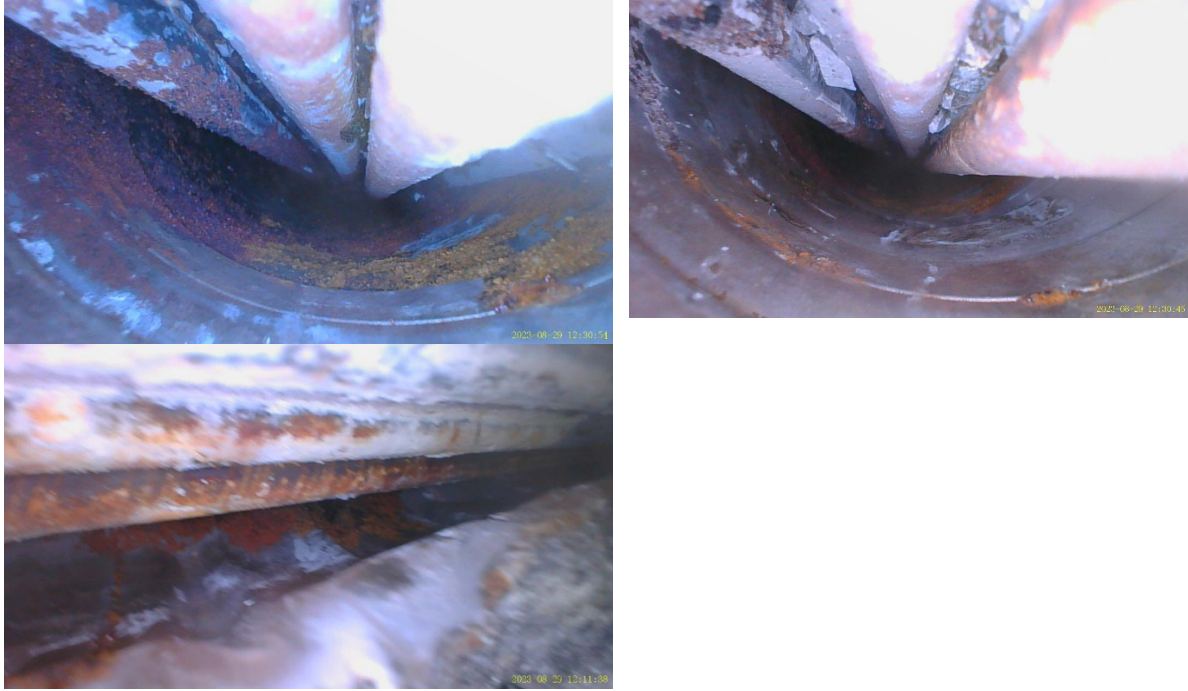
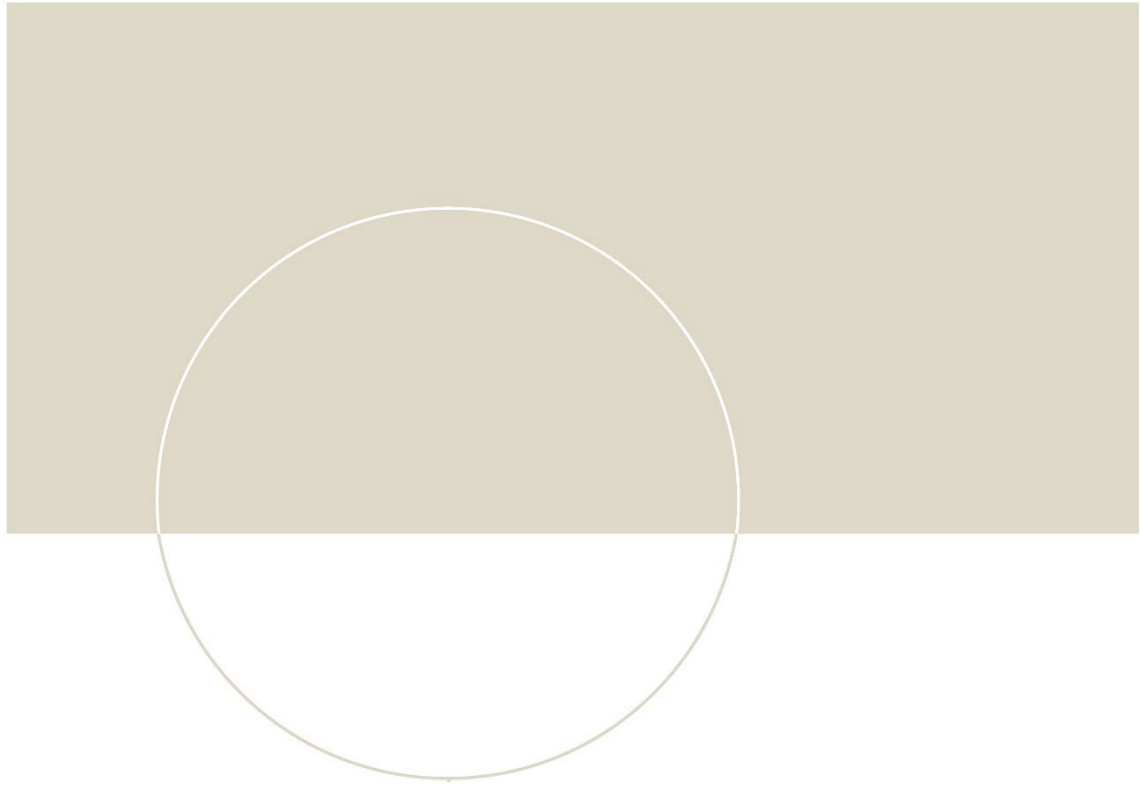


Figure E-3: 2SA Videoscope [7].



Figure E-4: 2SA-4 [7].



 **NTNU**

Norwegian University of  
Science and Technology